

# Approaching Thouless Energy and Griffiths Regime in Random Spin Systems By Singular Value Decomposition

Wen-Jia Rao\*

*School of Science, Hangzhou Dianzi University, Hangzhou 310027, China.*

(Dated: October 12, 2021)

We employ singular value decomposition to study the eigenvalue spectrums of random spin systems. It's shown the singular values  $\lambda_k$  of the sample matrix in the ergodic phase contain two branches that both follow power-law behavior but with different power exponents  $\alpha$ . By analyzing the singular vectors, it is verified the higher part of  $\lambda_k$  with  $k > k_{\text{Th}}$  are universal that follows random matrix theory, where  $k_{\text{Th}}$  estimates the Thouless energy. We further demonstrate that  $\alpha$  corresponds only to the exponential part of the level spacing distribution while is insensitive to the level repulsion, or equivalently the system's symmetry. Consequently, the power exponent  $\alpha$  gives an underestimation for the many-body localization transition point, which, however, reveals the Griffiths regime in a transparent way.

## I. INTRODUCTION

The quantum phases of matter in isolated systems is a focus of modern condensed matter physics, it has been well-established the existence of two generic phases: an ergodic phase and a many-body localized (MBL) phase<sup>1,2</sup>. In an ergodic phase, the system acts as the heat bath for its subsystem, which results in extensive quantum entanglement that follows volume-law. In contrast, a MBL phase is where localization persists in the presence of weak interactions, which leads to area-law entanglement. The different scaling behaviors of quantum entanglement provide the modern understanding about these two phases<sup>3-9</sup>.

On the other hand, the ergodic and MBL phase are traditionally distinguished by their eigenvalue statistics<sup>10-18</sup>, whose foundation is laid by the random matrix theory (RMT)<sup>19,20</sup>. RMT is a powerful mathematical tool that describes the universal properties of the eigenvalues in the ergodic phase which depend only on the system's symmetry while independent of microscopic details. Specifically, the Gaussian orthogonal/unitary ensemble (GOE/GUE) describes systems with/without time reversal symmetry, and Gaussian symplectic ensemble (GSE) stands for time-reversal invariant systems with broken spin rotational invariance. On the contrary, the eigenvalues in MBL phase are independent of each other and belongs to the Poisson ensemble.

Compared to the properties of each phase, the evolution between them is much less understood, especially on the ergodic side. There are two issues of particular interest. First one concerns the energy scale called Thouless energy  $E_{\text{Th}}$ , defined through the Thouless time  $t_{\text{Th}} = \hbar/E_{\text{Th}}$ , which measures the average time a particle takes to diffuse over the system. Therefore, eigenvalue fluctuations below  $E_{\text{Th}}$  are well characterized by RMT and hence universal, while those above  $E_{\text{Th}}$  are model dependent. This energy scale  $E_{\text{Th}}$  is difficult to observe with local spectral statistics such as level spacing or spacing ratio distributions, but can be probed by long-range spectral measures such as the number variance<sup>21-23</sup> or spectral form factor<sup>24-27</sup>. The second issue regards the Griffiths regime near the transition region<sup>29-33</sup>, where an inhomogeneous mixture of locally thermal and localized regions co-exist and result

in anomalously slow dynamics and multifractality of eigenstates. Unlike the Thouless energy, study of Griffiths effect is normally based on eigenfunctions.

In this work, we employ the singular-value-decomposition (SVD) to study the eigenvalue spectrums of random spin systems with MBL transition, and show that both the Thouless energy and Griffiths regime can be revealed through the scaling of singular values. The advantage of this method are twofolded. For the Thouless energy, SVD requires no unfolding procedure, which is necessary for studying number variance and spectral form factor, and therefore avoids the potential ambiguity raised by concrete unfolding strategy<sup>28</sup>. Very recently, Berkovits employed SVD to the study of Thouless energy in Anderson model<sup>22</sup> and the identification of non-ergodic extended phase in the Rosenzweig-Porter model<sup>23,34</sup>, and now we bring it to the many-body regime. For the Griffiths effect, the inputs of SVD are the eigenvalue spectrums, which are numerically much easier to obtain than the eigenfunctions.

The underlying mechanism behind SVD is to view the eigenvalue spectrum of a complex quantum system as a time-series<sup>35-38</sup>, and by performing SVD to the sample matrix (see Eq. (2) in Sec.II) we are able to distinguish the trend and fluctuation modes therein. This technique is in essence identical to the unsupervised machine learning algorithm called principal component analysis (PCA), which has also found applications in condensed matter physics<sup>39-42</sup>. However, while PCA deals with several components with largest weights, we shall see the universal information of MBL system is encoded in the intermediate components with lower weights.

This paper is organized as follows. In Sec. II we introduce the SVD method, and show the scree plot (singular values as a function of level index) for the MBL phase reflects a clear chaotic behavior, while that for the ergodic phase breaks into two branches – a universal high-order part that belongs to RMT and a non-universal part, with the starting point of the former identifying the Thouless energy  $E_{\text{Th}}$ . In Sec. III we dig into the structure of the principal components, and show the higher-order ones are close to the Fourier modes of the eigenvalue spectrum, which explains why the higher-order part of scree plot is universal. In Sec. IV we demonstrate the scree plot only reflects the exponential part of the spacing distribu-

tion while is insensitive to the level repulsion, or equivalently the system's symmetry. Consequently, as detailed in Sec. V, it gives an underestimation on the ergodic-MBL transition point, which, however, reflects the existence of Griffiths regime in a transparent way. Discussion and conclusion come in Sec. VI.

## II. SVD ON EIGENVALUE SPECTRUMS

In this work we consider the paradigmatic spin model with ergodic-MBL transition, that is, the anti-ferromagnetic Heisenberg model with random external fields<sup>43</sup>, the Hamiltonian reads

$$H_0 = \sum_{i=1}^L \mathbf{S}_i \cdot \mathbf{S}_{i+1} + \sum_{i=1}^L \sum_{\tau=x,y,z} h_\tau \varepsilon_i^\tau S_i^\tau, \quad (1)$$

where the coupling strength is set to be 1, and  $\varepsilon_i^\tau$ s are random variables within range  $[-1, 1]$ . We first consider the orthogonal case with time-reversal symmetry, that is,  $h_x = h_y = h \neq 0$  and  $h_z = 0$ , where an ergodic-MBL transition happens at  $h_c \simeq 3$ <sup>12,13</sup>. Using exact diagonalization, we generate  $N = 1000$  samples of eigenvalue spectrums at various randomness  $h$  in an  $L = 13$  system, with the Hilbert space dimension being  $2^{13} = 8192$ . For each spectrum, we take out the middle  $P = 1000$  eigenvalues, and arrange them into an  $N \times P$  sample matrix

$$X = \begin{pmatrix} E_1^{(1)} & E_2^{(1)} & \dots & E_P^{(1)} \\ E_1^{(2)} & E_2^{(2)} & \dots & E_P^{(2)} \\ \vdots & \vdots & \ddots & \vdots \\ E_1^{(N)} & E_2^{(N)} & \dots & E_P^{(N)} \end{pmatrix}, \quad (2)$$

where  $E_i^{(j)}$  stands for the  $m$ -th eigenvalue in the  $n$ -th sample. We then perform SVD on  $X$ , which equals to express  $X$  as

$$X = U\Lambda W \equiv \sum_k \sigma_k X^{(k)}, \quad (3)$$

where  $\Lambda$  is an  $N \times P$  matrix with positive diagonal elements being the ordered singular values  $\sigma_1 \geq \sigma_2 \geq \dots \geq \sigma_r$  with  $r \leq \min[N, P] = \text{Rank}[X]$ . With SVD,  $X$  can be decomposed into sum of components  $X_{ij}^{(k)} = U_{ik} W_{kj}$ , and  $W_k$  – the  $k$ -th row of the  $P \times P$  matrix  $W$  – denotes the  $k$ -th orthonormal basis (principal components) in the eigenvalue spectrum with weight  $\sigma_k$ . Given the decreasing tendency of  $\sigma_k$ ,  $X$  can be effectively approximated by  $\tilde{X} = \sum_{k=1}^m \sigma_k X^{(k)}$  with some value  $m$ . This is the essence of the statistical machine learning algorithm called principal component analysis (PCA), where only several dominant components are kept to represent the original data, hence achieving the purpose of dimension reduction. However, as we shall see, the universal information of the random spin system is encoded in the lower-weight components.

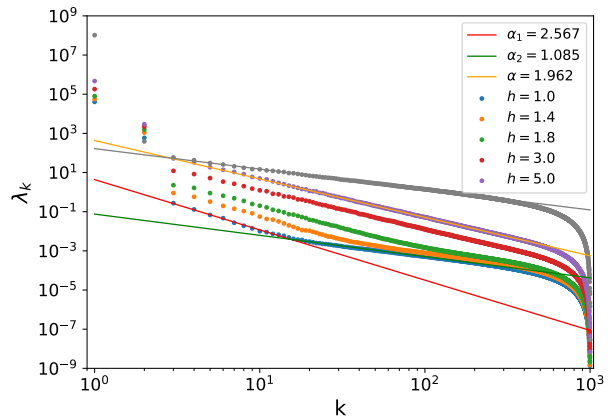


FIG. 1. Scree plots of  $\lambda_k$  at various randomness strengths. Despite the two dominant modes,  $\lambda_k$  in the MBL phase follows a power-law  $k^{-\alpha}$  with  $\alpha \simeq 2$  reflecting the integrable behavior. Two-branch structures appear for  $\lambda_k$  in the ergodic phase ( $h < 3$ ), separating the model-dependent lower part and the universal higher part that belongs to RMT, the starting point of the latter provides an estimation of the Thouless energy. The grey dots:  $\lambda_k$  from modeling GOE, with the power exponent being  $\alpha = 1.043$  reflecting its chaotic nature.

Another interpretation of SVD is to treat  $X$  as a multivariate time series, with  $\lambda_k \equiv \sigma_k^2$  being the eigenvalue of the covariance matrix  $X^T X$ . It has been demonstrated<sup>22,23,35,36</sup> that  $\lambda_k$  with large  $k$  follows the power-law behavior

$$\lambda_k \sim \frac{1}{k^\alpha} \quad (4)$$

with  $\alpha = 1$  (2) in the chaotic (integrable) system, corresponding to the ergodic (MBL) phase respectively.

As a demonstration, we collect the sample matrix  $X$  for Eq.(1) with  $L = 13$  at various randomness strengths, and plot the resulting  $\lambda_k$  after SVD with respect to the level index  $k$  (the so-called scree plot) in a log-log scale in Fig. 1. For comparison, we also generate eigenvalue spectrums from modeling GOE matrices (orthogonal matrices with random elements drawn from standard Gaussian distribution  $N(0, 1)$ ) of the same size, the resulting  $\lambda_k$  appear as the grey dots therein. Clearly, in all cases, the first two modes are orders of magnitudes larger than the rest, which stand for two broad features in the eigenvalue spectrum. For reasons detailed in next section, we identify them to be the mean energy  $\langle E \rangle$  and mean level spacing  $\langle s \rangle$ . While for large modes with  $k > 300$ , the weights drops very rapidly, indicating they contribute little to the properties of the eigenvalue spectrum. The universal information is thus expected to be encoded in the intermediate modes with  $2 < k < 300$ .

More specifically, for case in the MBL phase ( $h = 5$ ),  $\lambda_k$  with  $3 \leq k \leq 200$  fits well into the power-law behavior Eq.(4) with  $\alpha = 1.962$ , very close to the value 2 for integrable system as expected. While for data in the ergodic phase ( $h = 1$ ),  $\lambda_k$  divides into two parts: the higher-part  $30 \leq k \leq 200$  are fitted well with  $\alpha_2 \simeq 1.085$ , reflecting a clear chaotic behavior, this

part is identified to be universal below Thouless energy and related to RMT; the lower-part  $3 \leq k \leq 15$  follows a power-law behavior with  $\alpha_1 \simeq 2.567$ . Such a super-Poissonian behavior is absent in the scree plot of a pure GOE (the grey dots in Fig. 1), and is therefore identified to be the model-dependent part beyond Thouless energy. Interestingly, this value of  $\alpha_1$  happens to be close to the one in the metallic phase of a 3D Anderson model<sup>22</sup>. The starting point of the high-order part identifies the Thouless energy  $E_{\text{Th}}$  through  $k_{\text{Th}} \sim 30$ . The two-branch structure is general for data in ergodic phase. With growing randomness, the  $E_{\text{Th}}$  decreases, and the two branches gradually get mixed. At the transition point  $h \simeq 3$ , the scree plot becomes almost identical to that of the MBL phase, suggesting the saturation of  $\alpha_2$  may be an indicator for the MBL transition. However, as discussed in detail in Sec. V, this may not provide an accurate estimation.

Up to now, we have shown the first advantage of SVD, i.e. it provides an estimation of Thouless energy in a transparent way, without performing any unfolding procedure. To further pursue the physics behind the scree plot, we turn to the analysis of principal components  $W_k$ .

### III. PRINCIPAL COMPONENT ANALYSIS

The  $k$ -th principal component of the eigenvalue spectrum is encoded in the  $k$ -th row of the matrix  $W$ , we therefore draw the behavior of  $W_k$  with respect to the energy level index  $i$  to read out the physics. The results in this section are based on the sample matrix from  $h = 1$ , and we have checked they hold in other cases as well.

First of all, we draw the two dominant components  $W_1$  and  $W_2$  in Fig. 2(a), it's clear that both of them are linearly dependent with level index  $i$ , suggesting they correspond to (a linear combination of) two broad non-fluctuating features of the eigenvalue spectrum. The most natural guess for the two broad features would be the mean energy  $\langle E \rangle$  and spectrum's bandwidth, or equivalently the mean level spacing  $\langle s \rangle$ . To support this conjecture, we can change the input data from the eigenvalues  $\{E_i\}$  to the level spacings  $\{s_i = E_{i+1} - E_i\}$ . With this input, the information of mean energy  $\langle E \rangle$  is lost, leaving  $\langle s \rangle$  as the only dominant feature. Therefore when applying SVD to this new sample matrix  $X'$ , we should observe only one dominant component, which is verified in Fig. 2(b). To get rid of the information of  $\langle s \rangle$ , we can further change the input from level spacings  $\{s_i\}$  to spacing ratios  $\{s_{i+1}/s_i\}$ , and the resulting scree plot should contain no dominant components. As verified also in Fig. 2(b), it is indeed the case.

Strictly speaking, the mean energy  $\langle E \rangle$  and level spacing  $\langle s \rangle$  are non-universal for different reasons. The  $\langle E \rangle$  stands for the global energy scale of the system and hence depends on the model's details; while  $\langle s \rangle$  is the value that can be artificially assigned when counting level statistics (most commonly taken to be 1), which stems from the mathematical degree of freedom in the joint probability distribution function of the eigenvalues<sup>19,20</sup>.

Having understood the physics of the two dominant components, we now return to analysis of the higher components

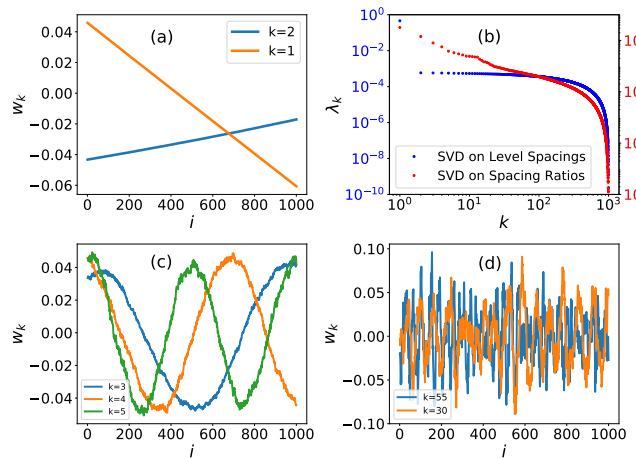


FIG. 2. (a) Behaviors of the two dominant components  $W_{1/2}$ , the linear behaviors indicates they correspond to two non-fluctuating features of the eigenvalue spectrum, which are suspected to be the mean energy  $\langle E \rangle$  and level spacing  $\langle s \rangle$ . (b) Scree plots of  $\lambda_k$  after performing SVD on the sample matrix comprised of level spacings and spacing ratios, the former contains only one dominant component while in the latter no dominant component appears. (c),(d) Behaviors of typical higher components  $W_k$ , the quasi-sinusoidal behaviors indicate they are close to the  $k$ -th Fourier mode of the eigenvalues, and the frequency increases with  $k$ .

$W_k$  ( $k \geq 3$ ) of the original sample matrix  $X$ , several of which are plotted in Fig. 2(c),(d). We observe clear sinusoidal behaviors of  $W_k$  with respect to level index  $i$ , with the frequency increasing with  $k$ . Specifically, we have  $W_k[i] \sim \cos\left(\frac{(k-1)\pi}{N}i + \varphi_k\right)$  with  $N = 1000$  being the number of eigenvalues, which indicates the mode  $W_k$  is close to the  $k$ -th Fourier mode of the eigenvalue spectrum. Therefore, for larger  $k$ ,  $W_k$  reflects the level fluctuations on shorter energy scale. In the ergodic phase, above certain value  $k_{\text{Th}}$ , this energy scale falls within Thouless energy and belongs to RMT. This is the origin of the two-branch structure of the scree plot in the ergodic phase, which also explains why the higher modes with smaller weights are universal.

Above arguments can be further supported. Given the (quasi) sinusoidal behaviors of  $W_k$ , the corresponding  $\lambda_k$  is close to the square of weight of the  $k$ -th Fourier mode of eigenvalue spectrum. This motivates us to perform the power spectrum analysis on the eigenvalue spectrum by considering

$$F_i(k) = \left| \frac{1}{r} \sum_{j=1}^r \left( \sum_{k=3}^r \sigma_k X_{ij}^{(k)} \right) \exp\left(-\frac{2\pi i k j}{r}\right) \right|^2, \quad (5)$$

where  $\sum_{k=3}^r \sigma_k X_{ij}^{(k)}$  are the eigenvalue spectrums that get rid of  $\langle E \rangle$  and  $\langle s \rangle$ , and can be viewed as the spectrums after global unfolding<sup>36-38</sup>. By averaging over the ensemble we get the power spectrum function  $F(k) = \frac{1}{N} \sum_{i=1}^N F_i(k)$ , which reveals the fluctuations of the eigenvalues. Therefore,  $F(k)$  is expected to follow the same power-law behavior as  $\lambda_k$ , that is  $F(k) \sim 1/k^\gamma$  with  $\gamma = \alpha$ . To this end, we calculate  $F(k)$  in

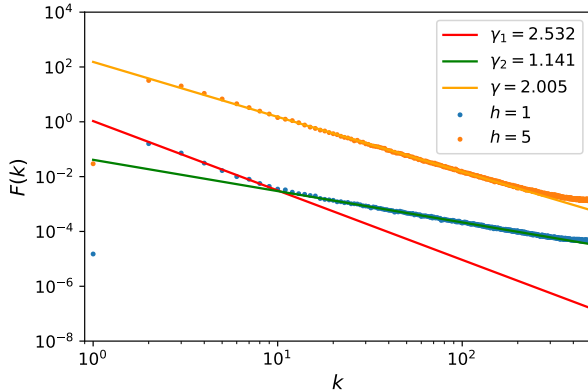


FIG. 3. Power spectrum  $F(k)$  for ergodic ( $h = 1$ ) and MBL ( $h = 5$ ) phases, in the former a clear two-branch structure appears just like in the scree plot of  $\lambda_k$ . The power exponents  $\gamma \simeq \alpha$  are observed as expected in all cases.

the  $h = 1$  (5) case standing for the ergodic (MBL) phase, the results are shown in Fig. 3. As we can see,  $F(k)$  in the ergodic phase falls into two parts that both follow  $1/k^\gamma$ , specifically, the lower modes satisfy  $\gamma_1 \simeq 2.5 \simeq \alpha_1$  and higher modes have  $\gamma_2 \simeq 1 \simeq \alpha_2$ . While for data in MBL phase, a single curve with  $\gamma \simeq 2 \simeq \alpha$  appears, as expected.

A technical issue worth mentioning is that the choice of power spectrum in Eq. (5) is not unique. Another routine, adopted in Ref.[35], is to construct the following time-series

$$\delta_n = \sum_{i=1}^n (s_i - \langle s \rangle) = s_n - n\langle s \rangle, \quad (6)$$

where  $s_n$  is the  $n$ -th order level spacing. It is clear that  $\langle \delta_n \rangle$  gets rid of the non-universal information about  $\langle E \rangle$  and  $\langle s \rangle$ , in a similar way to  $\sum_{k=3}^r \sigma_k X_{ij}^{(k)}$  in Eq. (5), hence its Fourier weight  $S(k)$  show totally similar behaviors to  $F(k)$  in Fig. 3.

#### IV. RELATING $\alpha$ TO LEVEL SPACING DISTRIBUTION

Up to now, we have demonstrated that the power-law exponent  $\alpha$  for  $\lambda_k$  with large  $k$  is universal that related to RMT. However, the power-law exponent  $\alpha$  is only a single number, it's still questionable whether it can distinguish different random matrix ensembles which may contain multiple parameters. For example, the general form of level spacing distribution  $P(s)$  contains two parts: the polynomial part that reflects the level repulsion, and an exponential part that reflects large  $s$  decaying. As for the random spin system, a widely-used two-parameter spacing distribution for the ergodic-MBL transition is proposed by Serbyn and Moore<sup>18</sup>, i.e.

$$P(\beta_1, \beta_2, s) = C_1 s^{\beta_1} \exp(-C_2 s^{2-\beta_2}). \quad (7)$$

For case deep in the ergodic phase, we have  $\beta_1 = 1, \beta_2 = 0$  standing for the GOE distribution; while for case deep in the

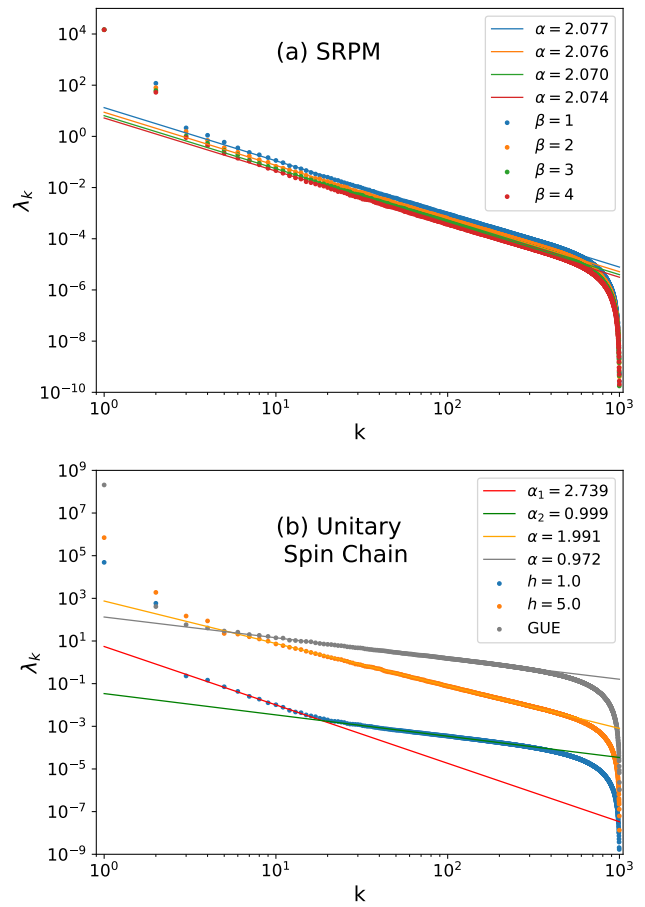


FIG. 4. (a) Scree plots of SRPM with different level repulsion  $\beta$ , the power exponent  $\alpha \simeq 2$  appears in all cases. (b) Scree plots for the unitary spin system, the behaviors of both the ergodic and MBL phases are totally similar to those in the orthogonal system, indicating the scree plot cannot distinguish the system's symmetry. Grey dots and line:  $\lambda_k$  from a modeling GUE.

MBL phase,  $\beta_1 = 0, \beta_2 = 1$  for the Poisson ensemble. We conjecture that the power exponent  $\alpha$  of  $\lambda_k$  corresponds *only* to the parameter  $\beta_2$  in the exponential part, while is insensitive to the level repulsion  $\beta_1$ . If this conjecture is correct, two deductions are immediate: (i) the scree plot with  $\alpha = 2$  does not necessarily correspond to the Poisson ensemble, but also to a number of intermediate ensembles whose spacing distribution decays as  $e^{-Cs}$ ; (ii) the scree plot with  $\alpha = 1$  in ergodic phase is insensitive to the level repulsion, or equivalently the symmetry of the system.

To verify (i), we consider the random matrix model called short-range plasma model (SRPM)<sup>48</sup>, which describes the eigenvalues as an ensemble of one-dimensional particles with only nearest neighboring logarithmic interactions. SRPM holds the semi-Poisson distribution which is widely accepted as the critical distribution at the MBL transition point. It is shown<sup>48</sup> that the large  $s$  behavior of SRPM decays as  $s^\beta e^{-(\beta+1)s}$  with  $\beta$  being the Dyson index controlling the strength of level repulsion. Thus, if the deduction (i) holds,

we should observe identical power-law exponents  $\alpha$  for cases with different  $\beta$ . To effectively obtain the eigenvalue spectrum of the SRPM, we make use of an elegant correspondence between SRPM and the Poisson ensemble, that is, the spectrum comprised of every  $(\beta + 1)$ -th eigenvalue from the Poisson ensemble is identical to the eigenvalue spectrum of SRPM with index  $\beta$ <sup>49</sup>. Therefore, we can easily obtain the sample matrix of SRPM to perform SVD, and the resulting scree plots for  $\beta = \{1, 2, 3, 4\}$  are displayed in Fig. 4(a). As expected, the scree plots are totally similar, and the power-law exponent  $\alpha \simeq 2$  appears in all cases, which verifies (i).

For deduction (ii), we consider a unitary spin system that breaks time-reversal symmetry, i.e. the case with  $h_x = h_y = h_z = h \neq 0$  in Eq. (1). This model undergoes an ergodic-MBL transition at around  $h_c \simeq 2.5$ <sup>12,13</sup>, with the level spacing distribution evolving from GUE to Poisson. We likewise take  $h = 1$  and  $h = 5$  to represent the ergodic and MBL phase respectively. With the same size of samples, we obtain the resulting scree plots shown in Fig. 4(b), where we also draw  $\lambda_k$  from a modeling GUE for comparison. As can be seen,  $\lambda_k \sim 1/k$  appears in both the higher part of ergodic phase and modeling GUE, which are totally similar to the ones in Fig. 1; and  $\lambda_k \sim 1/k^2$  appears for data in MBL phase as expected. These results indicate  $\alpha$  is insensitive to the system's symmetry, which verifies deduction (ii). Actually, the scree plots of Gaussian  $\beta$  ensembles with continuous  $\beta$  has been studied in Ref.[38], where  $\alpha \simeq 1$  is found in all cases even when  $\beta$  is very small.

## V. REVEALING THE GRIFFITHS REGIME

Given the universal information of the system is encoded in the power exponent  $\alpha_2$  of the higher part of the scree plot, it's a natural idea to employ it to detect the ergodic-MBL transition, without referring to the study of eigenfunctions. We expect the exponent  $\alpha_2$  to evolve from 1 in ergodic phase to 2 in MBL phase. Specifically, we consider the orthogonal spin model Eq. (1) with length  $L = 13$  in the randomness range  $h \in [1, 5]$  with interval  $\delta h = 0.2$ . We generate 1000 samples of eigenvalue spectrums at each  $h$ , and select 1000 eigenvalues in the middle to construct the sample matrix  $X$  and hence obtain  $\lambda_k$ . The exponent  $\alpha_2$  is determined by fitting  $\lambda_k \sim 1/k^{\alpha_2}$  for  $50 < k < 250$  in all cases.

For comparison, we employ another eigenvalue-based quantity to detect the MBL transition, that is, the inter-sample randomness, whose definition goes as follows. First, we adopt a variant definition of spacing ratio, which is<sup>10</sup>

$$t_i = \frac{\min\{s_{i+1}, s_i\}}{\max\{s_{i+1}, s_i\}}, \quad (8)$$

where  $s_i = E_{i+1} - E_i$  is the  $i$ -th level spacing. The mean value  $\bar{t}$  in different ensembles has been calculated to be<sup>44</sup>  $\bar{t}_{\text{GOE}} = 0.536$  and  $\bar{t}_{\text{Poisson}} = 0.386$ . The calculation of  $\bar{t}$  contains two steps: first we calculate the mean spacing ratio  $t_S = \langle t_i \rangle_{\text{samp}}$  in one sample, then we average  $t_S$  over an ensemble of samples to get  $\bar{t} = \langle t_S \rangle_{\text{en}}$ . The two steps generates two types of variance, the first one is  $V_S = \langle t_S^2 - \bar{t}^2 \rangle_{\text{en}}$ , i.e.

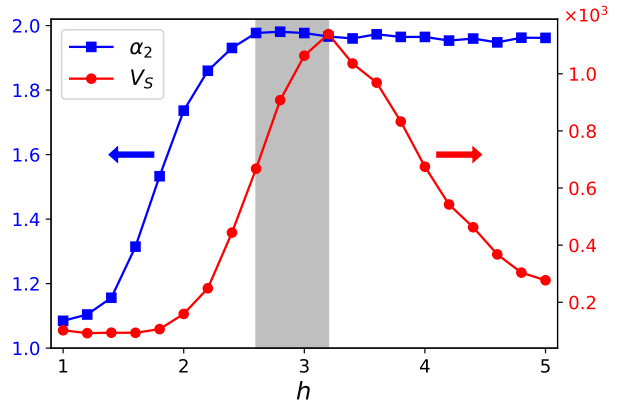


FIG. 5. Evolutions of  $V_S$  and the power law exponent  $\alpha_2$  with respect to the randomness strength  $h$ . The grey shaded area represents the Griffiths regime.

the variance of sample-averaged spacing ratio over ensemble, which measures the inter-sample randomness; another one is  $V_I = \langle v_I \rangle_{\text{en}}$  where  $v_I = \langle t_i^2 - t_S^2 \rangle_{\text{samp}}$ , measuring the intrinsic intra-sample randomness. In an MBL system driven by random disorder such as Eq. (1), the distribution of  $t_S$  near the transition region will deviate from a Gaussian function – a manifestation of Griffiths regime – which results in a peak of  $V_S$  at the transition point<sup>45–47</sup>. Therefore, we can compute the evolution of  $V_S$  to locate the transition.

The evolution of  $V_S$  and  $\alpha_2$  are drawn collectively in Fig. 5. The peak of  $V_S$  identifies the transition point to be  $h_c \simeq 3.2$ , which is very close to the widely accepted value  $h_c \simeq 3$ <sup>12,13</sup>, while  $\alpha_2$  saturates to 2 at roughly  $h = 2.6$ , smaller than the transition value. This result is consistent with the two-stage picture for the spacing distribution in Eq. (7) during MBL transition proposed by Serbyn and Moore<sup>18</sup>. Specifically, in the ergodic phase, there exists a finite Griffiths regime close to the transition point that contains locally localized small regions, which affects the large  $s$  decaying of  $P(s)$  more than the small  $s$  behavior. Consequently the parameter  $\beta_2$  increases to  $\beta_2 \sim 1$  even when the system is globally in the metallic phase. As demonstrated in previous section,  $\alpha_2$  detects only the power exponent in the exponential part of  $P(s)$  (that is,  $\beta_2$ ), it is not surprising that  $\alpha_2$  saturates earlier than the transition happens. In other words, the saturation of  $\alpha_2$  gives an underestimation for the transition point, and the finite region between the saturation and transition point (the shaded area in Fig. 5) reveals the Griffiths regime.

## VI. CONCLUSION AND DISCUSSION

We have employed the singular value decomposition (SVD) to study the eigenvalue spectrums of the random spin systems, and show the information of Thouless energy and Griffiths – both are of much current interest – can be revealed. By treating the eigenvalue spectrum as a time-series, we show the eigenvalue spectrum are dominated by two non-universal

features – the mean energy  $\langle E \rangle$  and level spacing  $\langle s \rangle$ , while higher component  $W_k$  ( $k \geq 3$ ) is close to the spectrum's  $k$ -th Fourier mode. Consequently, scree plot of the singular values  $\lambda_k$  in the ergodic phase exhibit two-branch structure: a non-universal lower-order part and a universal higher-order part, and the starting point of the latter gives an estimation for the Thouless energy. This approach requires no-unfolding procedure, which is necessary when studying number variance and spectral form factor.

On the other hand, we also improve the understanding about the power-law behavior of  $\lambda_k \sim 1/k^\alpha$ . By studying the scree plots of SRPM and a unitary spin chain, we verified the universal exponent  $\alpha$  corresponds only to the power-law parameter  $\beta_2$  in the exponential part of spacing distribution in Eq. (7) while is insensitive to the level repulsion parameter  $\beta_1$ , or equivalently the symmetry of the system. Consequently,  $\alpha$  gives an underestimation for the ergodic-MBL tran-

sition point, which, however, reveals the existence of Griffiths regime in a direct way.

The existence of subtle correspondence between the eigenvalues and eigenfunctions is an intriguing property of complex quantum system<sup>50</sup>, and there is certainly more hidden information in the eigenvalues deserves to be explored. One immediate direction is to construct an eigenvalue-based time series that is able to read the symmetry of the system (most probably through the level repulsion). It's also possible to apply SVD to non-Hermitian MBL systems with complex eigenvalues<sup>51,52</sup>, it's exciting to see whether such power-law scree plots appear in these systems or not.

## VII. ACKNOWLEDGEMENTS.

This work is supported by the National Natural Science Foundation of China through Grant No.11904069.

\* wjr@hdu.edu.cn

- <sup>1</sup> I. V. Gornyi, A. D. Mirlin, and D. G. Polyakov, Phys. Rev. Lett. **95**, 206603 (2005); **95**, 046404 (2005).
- <sup>2</sup> D. M. Basko, I. L. Aleiner, and B. L. Altshuler, Ann. Phys. **321**, 1126 (2006).
- <sup>3</sup> J. A. Kjall, J. H. Bardarson, and F. Pollmann, Phys. Rev. Lett. **113**, 107204 (2014).
- <sup>4</sup> Z. C. Yang, C. Chamon, A. Hamma, and E. R. Mucciolo, Phys. Rev. Lett. **115**, 267206 (2015).
- <sup>5</sup> M. Serbyn, A. A. Michailidis, M. A. Abanin, and Z. Papić, Phys. Rev. Lett. **117**, 160601 (2016).
- <sup>6</sup> M. Serbyn, Z. Papić, and D. A. Abanin, Phys. Rev. X **5**, 041047 (2015).
- <sup>7</sup> H. Kim and D. A. Huse, Phys. Rev. Lett. **111**, 127205 (2013).
- <sup>8</sup> J. H. Bardarson, F. Pollman, and J. E. Moore, Phys. Rev. Lett. **109**, 017202 (2012).
- <sup>9</sup> M. Serbyn, Z. Papić, and D. A. Abanin, Phys. Rev. B **90**, 174302 (2014).
- <sup>10</sup> V. Oganesyan and D. A. Huse, Phys. Rev. B **75**, 155111 (2007).
- <sup>11</sup> Y. Avishai, J. Richert, and R. Berkovits, Phys. Rev. B **66**, 052416 (2002).
- <sup>12</sup> N. Regnault and R. Nandkishore, Phys. Rev. B **93**, 104203 (2016).
- <sup>13</sup> S. D. Geraedts, R. Nandkishore, and N. Regnault, Phys. Rev. B **93**, 174202 (2016).
- <sup>14</sup> V. Oganesyan, A. Pal, D. A. Huse, Phys. Rev. B **80**, 115104 (2009).
- <sup>15</sup> A. Pal, D. A. Huse, Phys. Rev. B **82**, 174411 (2010).
- <sup>16</sup> S. Iyer, V. Oganesyan, G. Refael, D. A. Huse, Phys. Rev. B **87**, 134202 (2013).
- <sup>17</sup> D. J. Luitz, N. Laflorencie, and F. Alet, Phys. Rev. B **91**, 081103(R) (2015).
- <sup>18</sup> M. Serbyn and J. E. Moore, Phys. Rev. B **93**, 041424(R) (2016).
- <sup>19</sup> M. L. Mehta, *Random Matrix Theory*, Springer, New York (1990).
- <sup>20</sup> F. Haake, *Quantum Signatures of Chaos*, (Springer 2001).
- <sup>21</sup> B. Altshuler and B. Shklovskii, Sov. Phys. JETP [Zh. Eksp. Teor. Fiz. **91**,220] **64**, 127 (1986).
- <sup>22</sup> R. Berkovits, Phys. Rev. B **104**, 054207 (2021).
- <sup>23</sup> R. Berkovits, Phys. Rev. B **102**, 165140 (2020).
- <sup>24</sup> X. Chen and A. W. W. Ludwig, Phys. Rev. B **98**, 064309 (2018).

- <sup>25</sup> A. Chan, A. De Luca, and J. T. Chalker, Phys. Rev. Lett. **121**, 060601 (2018).
- <sup>26</sup> P. Sierant, D. Delande, and J. Zakrzewski, Phys. Rev. Lett. **124**, 186601 (2020).
- <sup>27</sup> J. Šuntajs, J. Bonča, T. Prosen, L. Vidmar, Phys. Rev. E **102**, 062144 (2020).
- <sup>28</sup> J. M. G. Gomez, R. A. Molina, A. Relano, and J. Retamosa, Phys. Rev. E **66**, 036209 (2002).
- <sup>29</sup> K. Agarwal, S. Gopalakrishnan, M. Knap, M. Müller, and E. Demler, Phys. Rev. Lett. **114**, 160401 (2015).
- <sup>30</sup> S. Gopalakrishnan, K. Agarwal, E. Demler, D. A. Huse, and M. Knap, Phys. Rev. B **93**, 134206 (2016).
- <sup>31</sup> K. Agarwal, E. Altman, E. Demler, S. Gopalakrishnan, D. A. Huse, and M. Knap, Ann. Phys., Lpz. **529**, 1600326 (2017).
- <sup>32</sup> D. J. Luitz and Y. Bar Lev, Ann. Phys., Lpz. **529**, 1600350 (2017).
- <sup>33</sup> N. Macé, F. Alet, and N. Laflorencie, Phys. Rev. Lett. **123**, 180601 (2019).
- <sup>34</sup> V. E. Kravtsov, I. M. Khaymovich, E. Cuevas, and M. Amini, New J. Phys. **17**, 122002 (2015).
- <sup>35</sup> A. Relano, J. M. G. Gómez, R. A. Molina, J. Retamosa, and E. Faleiro, Phys. Rev. Lett. **89**, 244102 (2002).
- <sup>36</sup> R. Fossion, G. Torres-Vargas, and J. C. López-Vieyra, Phys. Rev. E, **88**, 060902(R) (2013).
- <sup>37</sup> G. Torres-Vargas, R. Fossion, C. Tapia-Ignacio, and J. C. López-Vieyra, Phys. Rev. E, **96**, 012110 (2017).
- <sup>38</sup> G. Torres-Vargas, J. A. Méndez-Bermúdez, J. C. López-Vieyra, and R. Fossion, Phys. Rev. E, **98**, 022110 (2018).
- <sup>39</sup> L. Wang, Phys. Rev. B **94**, 195105 (2016).
- <sup>40</sup> C. Wang and H. Zhai, Phys. Rev. B **96**, 144432 (2017).
- <sup>41</sup> N. C. Costa, W. Hu, Z. J. Bai, R. T. Scalettar, and R. R. P. Singh, Phys. Rev. B **96**, 195138 (2017).
- <sup>42</sup> N. Jiang, S. Ke, H. Ji, H. Wang, Z.-X. Hu, and X. Wan, Phys. Rev. B **102**, 115140 (2020).
- <sup>43</sup> F. Alet and N. Laflorencie, C. R. Physique **19**, 498-525 (2018).
- <sup>44</sup> Y. Y. Atas, E. Bogomolny, O. Giraud, and G. Roux, Phys. Rev. Lett. **110**, 084101 (2013).
- <sup>45</sup> P. Sierant and J. Zakrzewski, Phys. Rev. B **99**, 104205 (2019).
- <sup>46</sup> V. Khemani, D. N. Sheng, and D. A. Huse, Phys. Rev. Lett. **119**, 075702 (2017).
- <sup>47</sup> W.-J. Rao, J. Phys. A: Math. Theor. **54**, 105001 (2021).

- <sup>48</sup> E. B. Bogomolny, U. Gerland and C. Schmit, *Eur. Phys. J. B* **19**, 121 (2001).
- <sup>49</sup> H. Hernández-Saldaña, J. Flores, and T. H. Seligman, *Phys. Rev. E* **60**, 449 (1999).
- <sup>50</sup> J. T. Chalker, Igor V. Lerner, and Robert A. Smith, *Phys. Rev. Lett.* **77**, 554 (1996).
- <sup>51</sup> R. Hamazaki, K. Kawabata, and M. Ueda, *Phys. Rev. Lett.* **123**, 090603 (2019).
- <sup>52</sup> L. Sá, P. Ribeiro, and T. Prosen, *Phys. Rev. X* **10**, 021019 (2020).